THE JOURNAL OF PHYSICAL CHEMISTRY B

Article

pubs.acs.org/JPCB

Stepwise Unfolding of Bovine and Human Serum Albumin by an Anionic Surfactant: An Investigation Using the Proton Transfer Probe Norharmane

Saptarshi Ghosh,[†] Satrajit Chakrabarty,[†] Debipreeta Bhowmik,[‡] Gopinatha Suresh Kumar,[‡] and Nitin Chattopadhyay*,[†]

[†]Department of Chemistry, Jadavpur University, Kolkata 700 032, India

[‡]Biophysical Chemistry Laboratory, Chemistry Division, CSIR-Indian Institute of Chemical Biology, Kolkata 700 032, India

Supporting Information

ABSTRACT: Interactions of the anionic surfactant sodium dodecyl sulfate (SDS) with the transport proteins bovine serum albumin (BSA) and human serum albumin (HSA) have been divulged using an external photoinduced proton transfer probe, norharmane (NHM). Steady-state fluorometry, time-resolved measurements, micropolarity analysis, circular dichroism (CD), and isothermal titration calorimetry (ITC) have been exploited for the study. With the gradual addition of SDS to the probe-bound proteins, the fluorometric responses of the different prototropic species of NHM exhibit an opposite pattern as to that observed while NHM binds to the proteins. The study reveals a sequential unfolding of the serum proteins with the gradual addition of SDS. ITC measures the heat changes associated with each step of the unfolding. ITC experiments, carried out at two different pH's, elucidate the nature of interaction between SDS and the two serum proteins. At a very high concentration of SDS, the external probe (NHM) is found to be dislodged from the protein environments to bind to the SDS micellar medium.

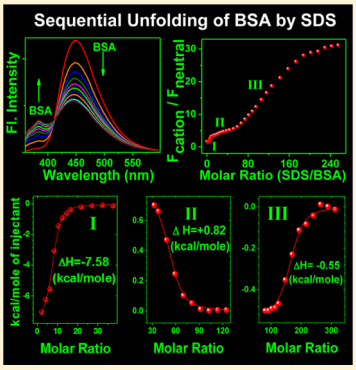

1. INTRODUCTION

Serum albumins (SAs) are the transport proteins abundantly present in the blood plasma, the main function of which is the transport and disposition of several endogenous and exogenous agents in the bloodstream to accomplish targeted delivery.[1,2] The primary structure of these transport proteins has about 580 amino acid residues and is characterized by a low content of tryptophan and a high content of cystine stabilizing a series of nine loops. The secondary structure of these serum albumins is constituted of ∼67% helix of 6 turns and 17 disulfide bridges.[1,2] The tertiary structure is composed of three domains, I, II, and III, with each domain being subdivided into two subdomains, A and B.[3,4] As domains II and III share a common interface, binding of a probe to domain III leads to conformational changes affecting the binding affinities to domain II and vice versa. Human and bovine serum albumins (HSA and BSA) display approximately 80% sequence homology and a repeating pattern of disulfides, which are strictly conserved. From the spectroscopic point of view, the main difference between the two proteins is that HSA has only one tryptophan residue (Trp-214), whereas BSA has two tryptophan residues (Trp-134 and Trp-212) at different positions.[3,4] From the crystallographic structure of HSA, it is proposed that in this protein the single tryptophan residue (Trp-214) is located in the subdomain IIA consisting of the Lys(212)-Ala(213)-Trp(214)-Ala(215)-Val(216)-Ala(217)-Arg(218) chain of the amino acid. In the case of BSA, Trp-212 is located in a similar microenvironment of subdomain IIA as the single Trp-214 in HSA, but Trp-134 is found to be localized in the second helix of subdomain IB, and buried in a hydrophobic pocket.[4] However, this assembling of the domains can be modified depending on the environmental conditions. Helms et al. and El-Kemary et al. have suggested that the serum proteins can adopt many conformations, ranging from a compact structure to a relaxed form.[5,6] Albumins have been identified as major transport proteins in blood plasma for many compounds like drugs, fatty acids, hormones, etc. Furthermore, albumins are the biomacromolecules that are involved in the maintenance of colloid-blood pressure and are implicated in facilitating transfer of many ligands across the organ−circulatory interfaces such as liver, intestine, kidney, and brain.[7] Fluorescence-probe spectroscopy of proteins is one of the most powerful methodologies, yielding structural and dynamical information concerning the fluorophore environment. Excited state photophysics is known to be exploited since long to explore the interaction between a fluorescent probe and its environment.[8−12] The structures of HSA and BSA are given in Scheme 1, showing different domains, subdomains, and the positions of the tryptophan units.

Special Issue: Photoinduced Proton Transfer in Chemistry and Biology Symposium

Received: February 1, 2014
Revised: March 25, 2014
Published: March 27, 2014

dx.doi.org/10.1021/jp501150p | J. Phys. Chem. B 2015, 119, 2090−2102

Scheme 1. Structures of (A) Human Serum Albumin and (B) Bovine Serum Albumin

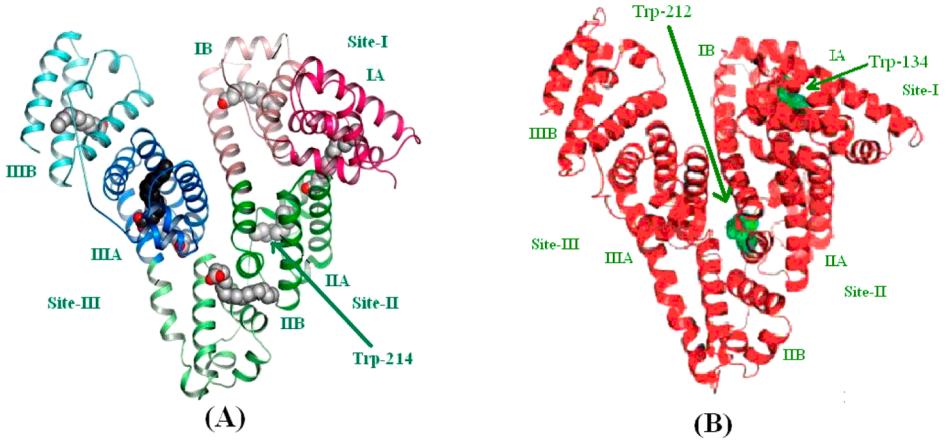

Norharmane (9*H*-pyrido[3,4-*b*-]-indole) (NHM) (Scheme 2) belongs to the group of naturally occurring bioactive alkaloids (*β*-carbolines) with a tricyclic pyrido (3,4-*b*) indole ring system that are found in about 26 plant families, foods, cells, animal tissues, and human urine. NHM has been shown to act as an efficient photosensitizer in the presence of oxygen to produce both the superoxide radical anion[13] and singlet oxygen.[14] It is also known that these compounds bind selectively with DNA[15] and form complexes with flavins.[16] Beljansky et al. have found that some *β*-carbolines can selectively and completely destroy the proliferative capability of various types of cancer cells upon excitation with UV radiation.[17]

Scheme 2. Different Acid−Base Equilibria for Norharmane[a]

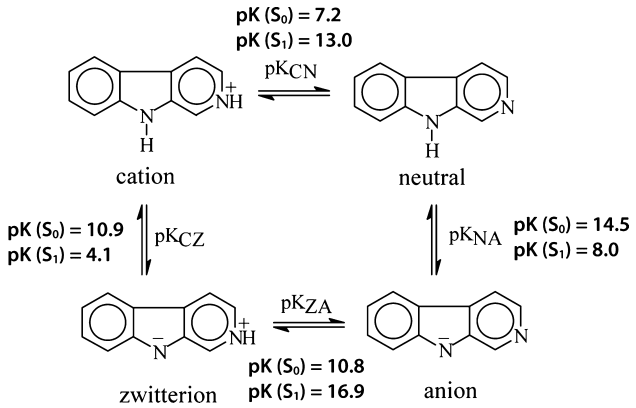

[a]CN, cation-neutral; NA, neutral-anion; ZA, zwitterion-anion; CZ, cation-zwitterion. The pK values are taken from ref 20.

Apart from the biological aspect, attention has also been focused on another important and interesting feature of norharmane, namely, its fluorescence from different prototropic species[18−20] that shows remarkable sensitivity to some parameters (e.g., polarity, pH, etc.) of the microenvironment. This has encouraged scientists to exploit this compound as a sensitive fluorescent molecular probe. The photophysics of this efficient cancer cell photosensitizer has been studied in different micellar environments of varying charges and chain lengths.[21,22] Formation of different types of inclusion complexes of NHM with cyclodextrins has also been established.[23] Chattopadhyay et al. have performed an extensive photophysical study on the binding interaction of NHM with the two most abundant model transport proteins, BSA and HSA.[24] They have shown that this biological photosensitizer, NHM, binds strongly to these two proteins with remarkable modification of its photophysical behavior.

Study of the interaction of proteins with small molecules, drugs, surfactants, and denaturants is an emerging topic of interest to scientists. Researchers are keen to discern the effect of the surfactant molecules on the structural aspects of the proteins. It is known that, at very high surfactant concentration, proteins get denatured; i.e., the three-dimentional structures of the proteins are destroyed. However, Takeda et al. suggested that HSA sustains its secondary structure up to 0.2 mM SDS.[25] Recently, Mukherjee et al. deciphered the microenvironment of the HSA−SDS assembly using steady-state and time-resolved fluorometric measurements.[26] They monitored the intrinsic fluorescence of the HSA coming from the tryptophan unit and proposed that binding of SDS to the protein occurs in a sequential manner. Although some studies exist on the effect of surfactant on the proteins, this area needs more attention to understand the protein−surfactant interaction more explicitly.

With this background, we have studied the effect of SDS on the two major transport proteins, i.e., BSA and HSA, using the prototropically sensitive biological fluorophore, NHM. Use of an external fluorophore label is already in vogue in the field of biophysical studies.[27] The steady-state and time-resolved fluorometric measurements along with CD spectroscopy have shown that gradual addition of SDS to the NHM−protein assembly causes a sequential unfolding of the serum proteins. Isothermal titration calorimetry (ITC) study strengthens this proposition of stepwise unfolding of proteins by the action of SDS and measures the amounts of heat changes in each step of unfolding. Our vivid investigation implies a three-step unfolding of the serum proteins with the gradual addition of SDS. ITC experiments at two different pH's reveal that the second phase of interaction between the serum proteins and SDS is hydrophobic in nature.

2. EXPERIMENTAL SECTION

2.1. Materials. BSA, HSA (both Sigma-Aldrich, USA), and HEPES (*N*-[2-hydroxyethyl]-piperazine-*N*′-[2-ethanesulfonic acid]) buffer (SRL, India) were used as received. Norharmane (NHM) procured from Sigma-Aldrich, USA, was purified by recrystallization from ethanol. 50 mM HEPES buffer solution was prepared, and its pH was adjusted to 7.0. The same buffer

dx.doi.org/10.1021/jp501150p | J. Phys. Chem. B 2015, 119, 2090−2102

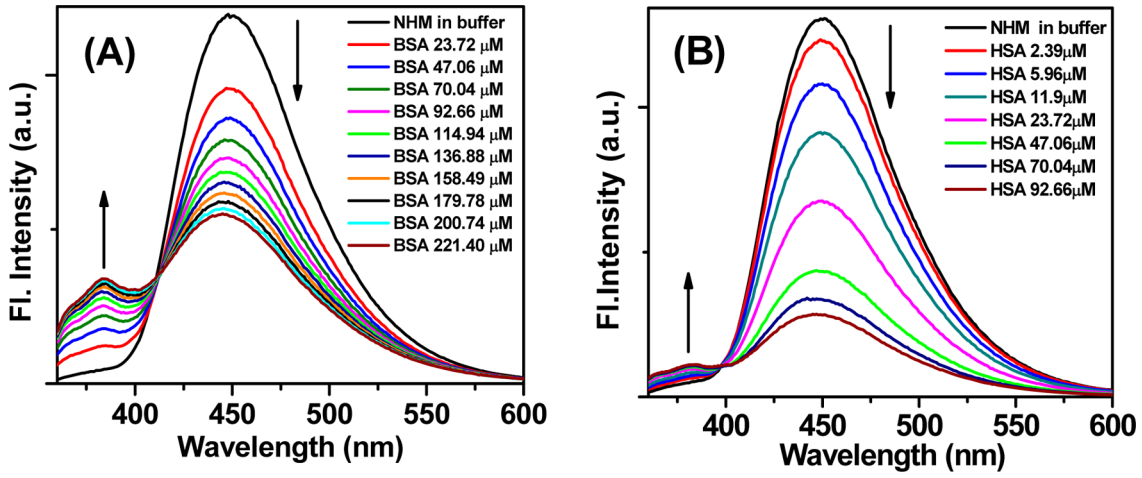

Figure 1. Emission spectra of NHM as a function of (A) BSA and (B) HSA concentration. λ_{exc} = 350 nm. The concentrations of the proteins are labeled in the legends.

solution was used as bulk medium throughout the experiment. Citric acid was procured from Merck, India, and used as received. A 25 mM citric acid buffer solution was prepared for ITC study in the lower pH region, and its pH was adjusted to 3.1. The surfactant sodium dodecyl sulfate (SDS) was used as procured (Fluka, USA). The micellar solutions were freshly prepared to avoid aging. Spectroscopic grade 1,4-dioxane (Spectrochem, India) was used for the polarity measurement experiments. Triple distilled water was used throughout the experiment. The fluorophore, NHM, was excited at 350 nm so as to excite principally the neutral species of NHM in the ground state.[20] The concentration of NHM was kept at ∼10 μM in all of the experiments.

2.2. Methods. A Shimadzu UV-2450 absorption spectrophotometer (Shimadzu Corporation, Kyoto, Japan) was used for the steady-state absorption studies. Steady-state fluorescence and fluorescence anisotropy measurements were performed with a Horiba Jobin Yvon Fluoromax-4 spectrofluorometer. Fluorescence anisotropy (r) is defined as

$$r = (I_{VV} - G \cdot I_{VH})/(I_{VV} + 2G \cdot I_{VH}) \quad (1)$$

where I_{VV} and I_{VH} are the emission intensities obtained with the excitation polarizer oriented vertically and emission polarizer oriented vertically and horizontally, respectively. The G factor is defined as[28]

$$G = I_{HV}/I_{HH} \quad (2)$$

where the intensities I_{HV} and I_{HH} refer to the vertical and horizontal positions of the emission polarizer, with the excitation polarizer being horizontal. All of the time-resolved measurements were performed on a Horiba−Jobin−Yvon FluoroCube fluorescence lifetime system using NanoLED at 370 nm (IBH UK) as the excitation source and TBX photon detection module as the detector. The decays were analyzed using IBH DAS-6 decay analysis software. The instrumental response time for our setup was ∼1 ns. The lamp profile was collected by placing a scatterer (dilute micellar solution of sodium dodecyl sulfate in water) in place of the sample. The goodness of fit was evaluated from χ^2 criterion and visual inspection of the residuals of the fitted function to the data. Mean (average) fluorescence lifetimes (τ_{avg}) for triexponential iterative fittings were calculated from the decay times (τ_1, τ_2, and τ_3) and the normalized pre-exponential factors (a_1, a_2, and a_3) using the following relation

$$\tau_{avg} = a_1\tau_1 + a_2\tau_2 + a_3\tau_3 \quad (3)$$

The circular dichroism spectra were recorded on a JASCO J-815 spectropolarimeter (Jasco International Co., Hachioji, Japan) using a rectangular quartz cuvette of path length 1 cm. The CD profiles were obtained employing a scan speed of 50 nm/min, and appropriate baseline corrections were made. All of the experiments were performed at room temperature (25 °C) with air-equilibrated solutions.

A Jencon (India) tensiometer was used for surface tension measurements by the ring detachment method. Sufficient time (5 min) was given prior to each measurement to allow thorough mixing and equilibration. Duplicate measurements were made to check reproducibility. A surface tension (γ) vs log[SDS] plot was used to get the CMC from the breaks in the plot.

Isothermal titration calorimetry (ITC) was performed on a MicroCal VP-ITC unit (MicroCal, Inc., Northampton, MA) using standard protocols,[29−31] at 25 °C, after electrical and chemical calibrations. BSA, HSA, and SDS solutions were degassed on the MicroCal's Thermovac unit prior to loading in order to avoid the formation of bubbles in the calorimeter cell. A total of 28 aliquots of degassed SDS (2 μL for the first 8 injections, 5 μL for the next 4 injections, 10 μL for the next 8 injections, and 20 μL for the last 8 injections) solution was injected from a rotating syringe (290 rpm) into the isothermal sample chamber containing the protein solution (1.4235 mL). The duration of each injection was 4 s for the first 8 injections, 10 s for the next 4 injections, 20 s for the next 8 injections, and 40 s for the last 8 injections, and the interval between each injection was 240 s. The initial delay before the first injection was 60 s. Corresponding control experiments to determine the heat of dilution of the surfactant were performed by injecting an identical volume of the same concentration of the surfactant into the buffer. The area under each heat burst curve was determined by integration using Origin 7.0 software to give the measure of the heat associated with the injections. The heat associated with each surfactant−buffer mixing was subtracted from the corresponding heat of surfactant−protein reactions to give the heat of the surfactant−protein interaction. The resulting corrected injection heats were plotted as a function

dx.doi.org/10.1021/jp501150p | J. Phys. Chem. B 2015, 119, 2090−2102

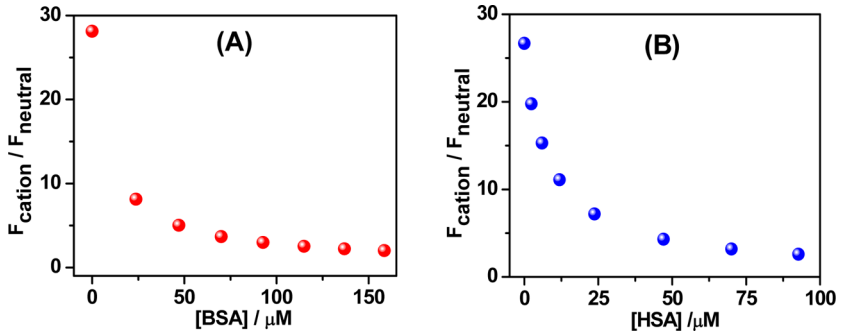

Figure 2. Variation of relative emission intensities of the cationic to the neutral species of NHM as a function of the concentration of (A) BSA and (B) HSA.

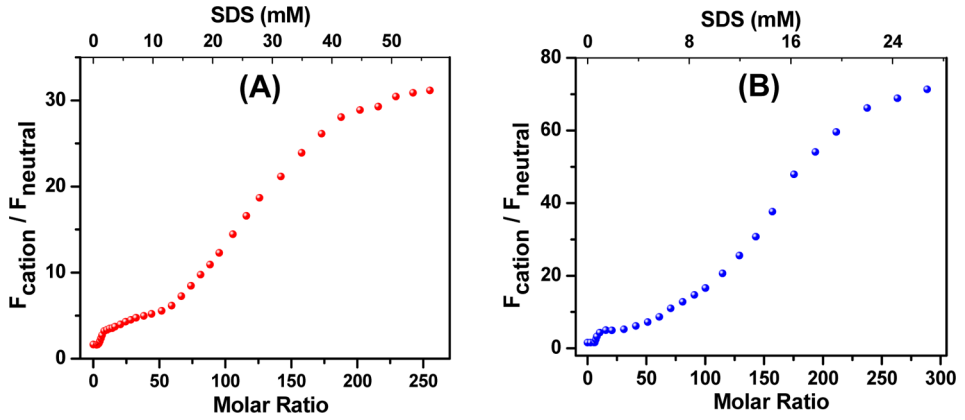

Figure 3. Plot of the ratio of emission intensities of cationic to neutral species of NHM in (A) BSA and (B) HSA as a function of the molar ratio of the added SDS to the protein and SDS concentration.

of the molar ratio, fit with a model for one set of binding sites, and analyzed using Origin 7.0 software.

3. RESULTS AND DISCUSSION

3.1. Steady-State Absorption and Emission Studies. The absorption spectrum of NHM in HEPES buffer solution at pH 7.0 shows two bands with maxima at 348 and 372 nm corresponding to the neutral and cationic species, respectively.[20] Addition of BSA or HSA to the aqueous buffered solution of NHM hardly changes the absorption spectrum. The emission spectrum of NHM in HEPES buffer shows a single and unstructured band peaking at 450 nm, ascribed to the cationic species of the NHM.[20,21] Gradual addition of the two aforesaid proteins, i.e., BSA and HSA, to the buffered solution of NHM changes the emission spectrum drastically. A new blue-shifted structured emission band with a peak at ∼380 nm develops at the cost of the emission corresponding to the cationic species at 450 nm, resulting in an isoemissive point at 410 nm for BSA and 398 nm for HSA. Figure 1 depicts the emission spectra of NHM as a function of BSA and HSA concentrations. In tune with the existing literature, the structured 380 nm band has been ascribed to the neutral species of NHM.[20] A plot of the ratio of the fluorescence intensities of cationic to neutral species of NHM ($F_{cation}/F_{neutral}$) against the concentration of the proteins shows, in a better way, the nature of variation in the fluorescence behavior of NHM with the addition of the proteins (Figure 2). The fluorometric behavior of NHM in the protein environment can be rationalized considering the prototropic character of the probe as well as the micropolarity−microproticity around the fluorophore within the proteinous environments.[32] As is evident from Figure 1, compared to the situation in the BSA environment, in HSA there is a greater drop of fluorescence intensity of the cationic species of NHM, while the appearance of the neutral band is rather less prominent. A stronger binding of NHM with HSA as compared to that with BSA might be responsible for a greater degree of fluorescence quenching of the cationic species of NHM in HSA.[24] A low fluorescence quantum yield of the neutral species of NHM in the HSA environment or energy transfer between NHM and albumins through some unidentified mechanism might be responsible for the other part of this observation. Further studies are invited before offering an unequivocal rationalization.

Addition of SDS to the probe-bound proteins results in a decrease in the emission intensity of the neutral band with a concomitant increase in the cationic band. Thus, with the addition of SDS, emission intensities of the neutral and cationic species of NHM behave in a reverse manner as to that observed while going from aqueous buffer to the protein environments. As done earlier, for a better understanding of the variation of relative intensities of the two aforesaid species of NHM, we have plotted $F_{cation}/F_{neutral}$ against the molar ratio of added SDS to the protein (Figure 3).

The striking feature of Figure 3 is that we observe a stepwise increase of the ratio of the fluorescence intensities of cationic to neutral species of NHM ($F_{cation}/F_{neutral}$) with increasing molar ratio of SDS to the proteins, contradictory to the gradual descending nature of $F_{cation}/F_{neutral}$ of NHM in Figure 2. Recently, Mukherjee et al. have reported a similar type of sequential fluorometric behavior of HSA with the gradual

dx.doi.org/10.1021/jp501150p | J. Phys. Chem. B 2015, 119, 2090−2102

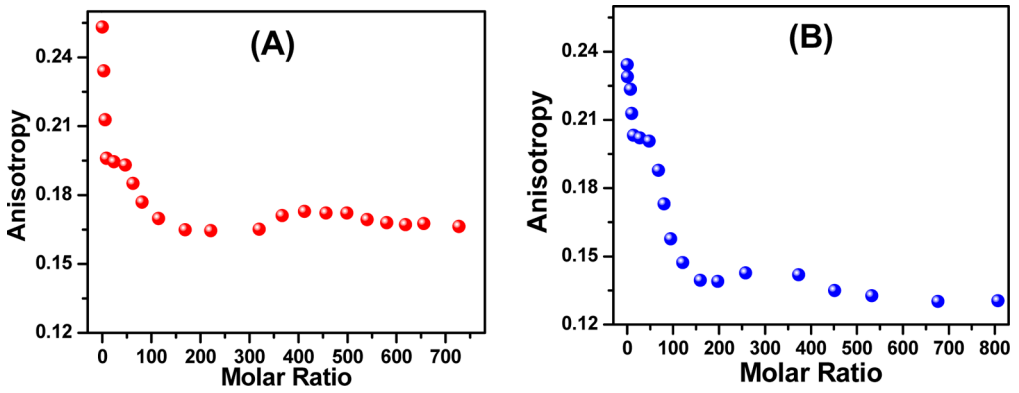

Figure 4. Variation of fluorescence anisotropy (r) of NHM bound to (A) BSA and (B) HSA with increasing molar ratio of SDS to protein. λ_{em} is 380 nm for both proteins.

addition of SDS exploiting the intrinsic fluorescence of HSA.[26] Observation of these distinct breakpoints for both of the serum proteins (Figure 3) implies that the proteins undergo structural unfolding by the action of SDS in a sequential manner. Sequential unfolding of HSA, induced by GdnHCl, has also been observed by Panda et al.[33] Figure 3 reveals that, at very low SDS concentration, i.e., up to a molar ratio of 5, for both of the proteins, we do not observe any noticeable change in the $F_{cation}/F_{neutral}$ value of NHM. That indicates the structure of the proteins remains unaltered in the lower range of SDS concentration, which is supported by the study of Moriyama and Takeda.[25] As a result of that, NHM remains bound in the protein and its fluorescence behavior is hardly affected in this range of concentration of the surfactant. On increasing the SDS concentration, we observe a sharp increase in the $F_{cation}/F_{neutral}$ value of NHM. In this region, binding of SDS monomers occurs to the specific high energy sites of proteins,[34−37] dislodging some bound NHM from the protein. Elimination of the probe from the less polar region in the probe−protein assembly to the more polar bulk aqueous medium causes stabilization of the cationic species of NHM,[32] and hence, a sharp increment in the $F_{cation}/F_{neutral}$ value of NHM occurs that continues up to a value of 15 of the molar ratio of SDS to the protein. Upon increasing the SDS concentration beyond the value of molar ratio 15, the $F_{cation}/F_{neutral}$ value rises up slowly and this continues until a molar ratio value of around 50 for both proteins. In this region, the bound SDS molecules may not meaningfully affect the binding of other SDS molecules to the proteins due to the long distance of binding sites. The binding in this region is termed as noncooperative binding.[34−37] Beyond the molar ratio 50, again we observe a sharp increase in the $F_{cation}/F_{neutral}$ value with further addition of SDS. This region corresponds to a massive change in binding caused by the cooperative interaction of SDS molecules with already bound SDS molecules. With more increase in SDS concentration, the $F_{cation}/F_{neutral}$ value saturates, suggesting that all protein-bound NHM molecules are eliminated from the protein due to structural unfolding of the protein. Thus, the stepwise increment of the $F_{cation}/F_{neutral}$ value of NHM with increasing SDS concentration dictates the sequential structural unfolding of the two serum albumins by the action of the anionic surfactant, SDS.

3.2. Steady-State Fluorescence Anisotropy Measurements. Steady-state fluorescence anisotropy reflects the extent of restriction imposed by the microenvironment on the dynamic properties of the probe, and hence can be exploited in assessing the motional information in the microheterogeneous environments.[24,28] An increase in the rigidity of the surrounding environment of a fluorophore results in an increase in the fluorescence anisotropy. We have monitored the fluorescence anisotropy as a function of protein concentration for both of the fluorescence bands of NHM (at 380 and 450 nm corresponding to the neutral and cationic species, respectively). The fluorescence anisotropy monitoring at 450 nm shows almost no change in both of the proteins (Figure S1 in the Supporting Information). This suggests that the cationic species resides in the bulk aqueous environment even in the presence of the albumins. The fluorescence anisotropy monitoring the neutral species (at 380 nm), however, shows a marked increase on moving from the aqueous phase to the protein environments, revealing that the rotational diffusion of the neutral form of the probe molecule is restricted significantly. The variation of fluorescence anisotropy (r) of the 380 nm emission of NHM as a function of protein concentration for both HSA and BSA is presented in the Supporting Information (Figure S2).

With gradual addition of SDS to the probe-bound proteins, the anisotropy value decreases to a value of 0.16 for BSA and 0.13 for HSA (Figure 4), which indicates the probe experiences lesser motional restriction with the introduction of SDS than that in protein environments. This decrement of the anisotropy value can be rationalized from the structural unfolding of the proteins by the action of SDS. As the proteins get unfolded, the bound probe is loosened and experiences lesser motional restriction than in the protein-bound condition. It is pertinent to mention here that the decrement of anisotropy exhibits a sequential pattern with increasing concentration of SDS similar to the observation in steady-state emission study. Another significant observation is that, when the proteins are largely unfolded at a very high concentration of SDS, anisotropy values of the probe do not come down to the value that is observed in the buffer, i.e., 0.04. This seems reasonable considering the fact that, though the proteins are unfolded, the medium remains sufficiently viscous to impose more motional restriction on the probe than that of the buffer.

3.3. Time-Resolved Fluorescence Decay Study. Fluorescence lifetime measurement serves as a tool to explore the local environment of the fluorophore within microheterogeneous environments, and it is sensitive to excited state interactions.[38,39] It also contributes to the understanding of the interactions between the probe and the proteins.[12] With the objective to see how the fluorescence lifetime of NHM is

dx.doi.org/10.1021/jp501150p | J. Phys. Chem. B 2015, 119, 2090−2102

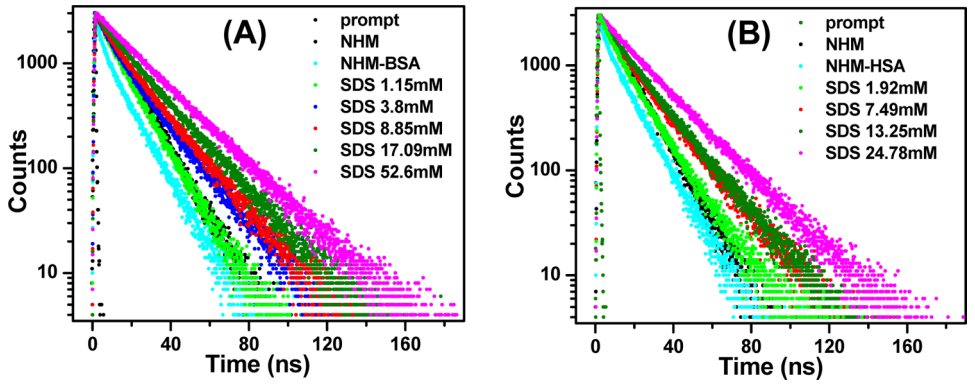

Figure 5. Time-resolved fluorescence decays of NHM in (A) BSA and (B) HSA and different SDS media (λ_{exc} = 370 nm). The sharp profile on the left is the lamp profile. The concentrations of the SDS media are labeled in the legends.

Table 1. Lifetime Values of NHM in Buffer, BSA, and Different SDS Media (λ_{em} = 450 nm)

solution	τ_1 (ns)	a_1	τ_2 (ns)	a_2	τ_3 (ns)	a_3	τ_{avg} (ns)	χ^2
buffer	12.48							1.05
BSA	12.78	0.25	3.44	0.18	0.69	0.57	4.19	1.03
[SDS] (mM)								
1.15	13.08	0.84	4.16	0.16			11.68	1.02
1.51	13.49	0.78	4.87	0.22			11.56	1.02
3.8	18.85	0.56	6.91	0.44			13.57	1.01
8.85	19.79	0.64	6.68	0.36			15.09	1.08
17.09	21.82	0.75	10.52	0.25			18.98	1.09
26.72	23.80	0.86	11.39	0.14			22.04	1.09
46.38	23.63							1.13

Table 2. Lifetime Values of NHM in Buffer, HSA, and Different SDS Media (λ_{em} = 450 nm)

solution	τ_1 (ns)	a_1	τ_2 (ns)	a_2	τ_3 (ns)	a_3	τ_{avg} (ns)	χ^2
buffer	12.52							1.09
HSA	12.45	0.26	2.77	0.16	0.47	0.58	6.99	1.03
[SDS] (mM)								
1.92	14.6	0.68	5.51	0.32			11.70	1.13
4.74	18.36	0.61	6.16	0.39			13.65	1.26
7.49	18.67	0.70	6.23	0.30			14.95	1.21
9.74	18.73	0.68	6.77	0.32			14.92	1.04
13.25	19.77	0.68	9.24	0.32			16.42	1.11
17.92	22.29	0.74	12.12	0.26			19.63	1.07
24.78	23.43	0.82	11.94	0.18			21.40	1.04
38.5	23.70							1.02

affected as the molecules move from the bulk aqueous phase to the proteins and upon subsequent addition of SDS, we have performed the fluorescence decay measurements. In buffer, at pH 7, the 450 nm emission of NHM exhibits a single-exponential decay with a lifetime of around 12.5 ns,[40] but in the protein environments, the decay of NHM becomes multi-exponential. Multiexponential decay of the fluorescence is quite common, even for chromophores in homogeneous environments, and it is often difficult to assign mechanistic models to explain the various components of the decay. The multi-exponential decay of a polarity-sensitive probe molecule may originate from the location of the probe in different polarity regions.[24] When SDS is added to the probe-bound protein, the decay pattern of the probe changes remarkably and at sufficiently high SDS concentration the probe shows a single-exponential decay. Typical decay profiles of NHM in the two protein environments and upon successive addition of SDS are shown in Figure 5, and the deconvoluted data are represented in Tables 1 and 2.

A glance at Tables 1 and 2 reflects that two of the lifetime values (τ_2 and τ_3) are observed in the protein environment to be lower than those measured in aqueous buffered solution, while the remaining component (τ_1) is of the same order as obtained in free buffered solution. Thus, the τ_1 component may be assigned to the free (not bound to protein) probe molecule. The data further show that with the addition of SDS to the protein-bound probe the lifetime components τ_1 and τ_2 increase. τ_1 reaches a value of ∼23 ns which is observed for NHM in SDS micellar medium,[22] and τ_2 reaches a value of ∼12 ns which is observed in aqueous buffered solution. Thus, the lifetime values of NHM imply that at very high SDS concentration the proteins are unfolded sufficiently and the bound probe comes out of the protein environment. Values of pre-exponential factors (a_1 and a_2) at a high concentration of SDS further suggest that a major part of the probes move in the

dx.doi.org/10.1021/jp501150p | J. Phys. Chem. B 2015, 119, 2090−2102

SDS micellar medium. It is pertinent to point out here that the long lifetime component of the probe (τ_1, Tables 1 and 2) begins to increase much more rapidly at around 4 mM SDS with both of the serum albumins in the buffer solution. This is ascribed to the incorporation of the HEPES molecules within the micelles. To establish that the HEPES buffer really modifies the CMC of the SDS system, we have independently determined the CMC values of SDS in aqueous as well as HEPES buffer solutions (Figure S3 in the Supporting Information) using the well-known ring detachment method. The determined CMC value of SDS in HEPES milieu comes out to be 4.47 mM compared to the CMC value of 8.28 mM in pure water.[41] Thus, the micelle formation in the buffer medium at a lower SDS concentration is responsible for the appreciable increase in the τ_1 of NHM in both the buffered BSA and HSA media. To understand the type of unfolding of the two proteins, we have plotted the mean fluorescence lifetime against the molar ratio of SDS to the protein (Figure S4 in the Supporting Information). Figure S4 (Supporting Information) implies that the average lifetime of the probe increases in a stepwise fashion, consistent with the sequential unfolding of the serum proteins.

3.4. Micropolarity Study. The study has been performed to inspect the polarity in the immediate vicinity of the fluorophore NHM under different situations. Polarity sensitive NHM fluorescence has made it a convenient tool for the determination of polarity of the microenvironment around the probe within the microheterogeneous environments.[24] The micropolarities in such environments are often determined and expressed in the equivalent $E_T(30)$ scale based on the transition energy for the solvatochromic intramolecular charge transfer absorption of the betaine dye 2,6-diphenyl-4(2,4,6-triphenyl-1-pyridono)phenolate, as developed by Kosower and Reichardt[42,43] comparing the fluorescence behavior of the probe in the microheterogeneous environments to that in a series of homogeneous solvent mixtures of varying composition with known $E_T(30)$ values. For this purpose, we have studied the fluorescence behavior of NHM in water−dioxane mixtures of varying composition.[44,45] The $E_T(30)$ values for different compositions of the dioxane−water mixtures are taken from the work of Kosower et al.[42] The inset of Figure 6 reveals that, with an increase in the water proportion in the water−dioxane solvent mixture, the emission intensity of the cationic species increases at the cost of the emission corresponding to the neutral species. This denotes that as the polarity of the microenvironment around the probe is enhanced the prototropic equilibrium moves toward the cationic species, resulting in an increase in the cationic band and a decrease in the band corresponding to the neutral species. A linear correlation is obtained from the plot of the logarithm of the ratio of the peak intensities of the neutral to cationic species ($\log(F_n/F_c)$) of NHM, using different compositions of water−dioxane mixtures for which $E_T(30)$ values are known (Figure 6). Comparing the value of the logarithm of the ratio of the band intensities of NHM in the two protein environments and with added SDS with the above correlation, we have determined the micropolarities around the probe at different situations (Figure 7). Figure 7 reveals that upon binding with both of the serum albumins the micropolarity of the probe decreases significantly and gradual addition of SDS to the protein-bound probe increases the micropolarity around the probe. Thus, this study suggests that SDS causes structural unfolding of the proteins, resulting in the release of the bound probe. It is pertinent to mention here that at very high SDS concentration, though the probe is completely eliminated from the probe−protein assembly, it cannot reach the micropolarity value that is observed in aqueous buffer. This can be attributed to the fact that, after being eliminated from the probe−protein assembly, the probe moves in the SDS micellar medium which is less polar than that of aqueous buffer and the micropolarity around the probe in the micellar medium should be less than that of the aqueous phase. In order to investigate the variation pattern of the micropolarity around NHM with added SDS, we have plotted the $E_T(30)$ value of the probe against the molar ratio of SDS to the proteins (Figure S5 in the Supporting Information). Like all other experiments already discussed, Figure S5 (Supporting Information) suggests that the micropolarity value of NHM does not vary in a continuous fashion with added SDS but rather it follows a sequential pattern.

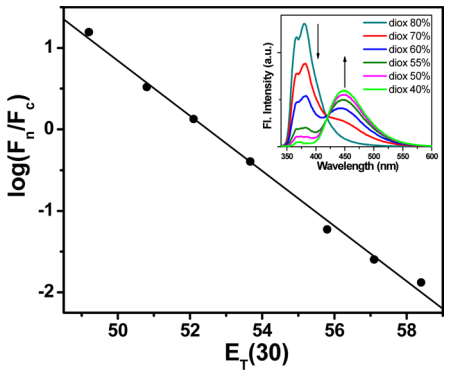

Figure 6. Variation of the log of the fluorescence yield of neutral to cationic species of NHM in a water−dioxane mixture against $E_T(30)$. The inset shows the emission spectra of NHM in a water−dioxane mixture under the same experimental condition (λ_{exc} = 350 nm). The volume percentages of dioxane in the water−dioxane mixtures are labeled in the legends.

3.5. Circular Dichroism Study. Circular dichroism (CD) spectroscopy is widely used to monitor the structure, conformation, and stability of proteins.[25,46,47] CD probes the secondary structure of proteins because the peptide bond is asymmetric and molecules without a plane of symmetry exhibit the phenomenon of CD. However, it does not provide the details regarding the precise structure of the proteins. Fluorescence techniques are more sensitive in deciphering small changes at the molecular level.[26] In order to decipher the structural and conformational changes, if any, brought in by the added SDS molecules, we have performed the CD spectral studies of the serum albumins bound with the probe in the presence of varying concentrations of the surfactant. Consistent with the literature, the CD spectra of both BSA and HSA show two minima at 208 and 222 nm (Figure 8), which is a signature of the presence of α-helix in both of the proteins under study.[25,47] The superimposed CD spectra of the proteins in the absence and in the presence of the probe reveal that, at least in the experimental concentration range, there is no detectable structural change of the proteins upon binding with the probe. A similar observation was also reported by Sengupta and Sengupta.[48]

Addition of SDS to the probe-bound proteins introduces a significant change in the CD spectra for both of the proteins, implying that, with the introduction of SDS, the proteins lose their structural rigidity. Although high concentrations of SDS

dx.doi.org/10.1021/jp501150p | J. Phys. Chem. B 2015, 119, 2090−2102

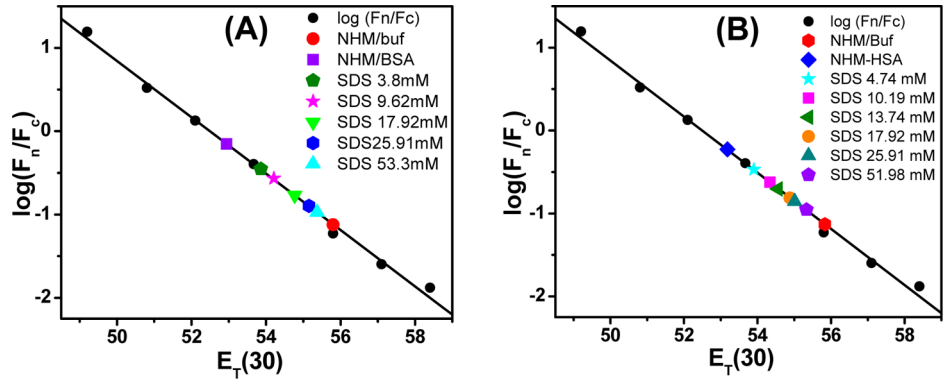

Figure 7. Variation of the logarithm of the ratio of the fluorescence yield of neutral to cationic species of NHM in a water−dioxane mixture: (A) BSA; (B) HSA and different SDS media against $E_T(30)$. The concentrations of the SDS media are labeled in the legends.

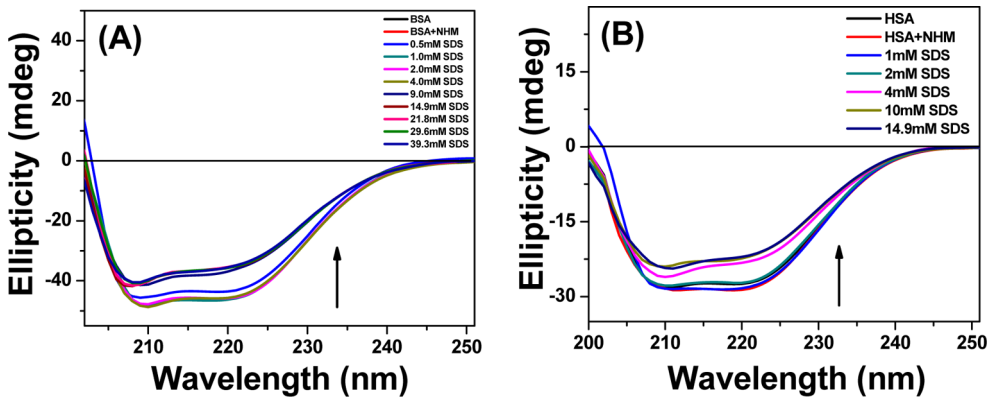

Figure 8. Circular dichroism spectra of (A) BSA and (B) HSA in various SDS concentrations. Concentrations are labeled in the legends.

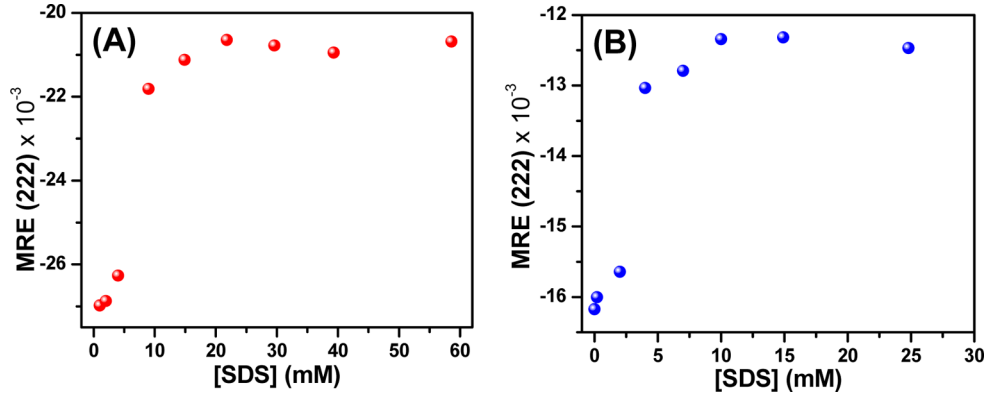

Figure 9. Plot of mean residue ellipticity (MRE) of (A) BSA and (B) HSA at 222 nm against [SDS].

bring about structural unfolding of HSA, it has been proposed that the helical structure remains almost 90% intact.[47] This clearly suggests that, even in the presence of high concentrations of SDS, the disulfide bonds are not completely broken or reduced, as proposed by Takeda and Moriyama.[49] It is important to remember that the CD results only give us an estimate of the global structural changes induced by the surfactant and surely do not provide us with the details of the microenvironmental changes induced. In order to investigate the effect of the added SDS on the structure of the proteins, we have plotted MRE222 (mean residual ellipticity at 222 nm) against the concentration of SDS, as shown in Figure 9. From Figure 9, it is evident that for both of the proteins helicity changes quite rapidly with added surfactant up to a SDS concentration of 20 mM. At high SDS concentration, binding of SDS to the protein surfaces leads to swelling of the proteins, resulting in breaking of the α-helices to give more open distorted structures. Beyond a SDS concentration of 20 mM, there is hardly any change in the secondary structure of the proteins, implying that proteins have lost their secondary structure significantly. It is pertinent to mention here that absorption by molecular oxygen below 210 nm will distort the CD spectra to some extent. However, this is not supposed to affect our overall interpretation, since we are monitoring the relative changes of the CD spectra of serum proteins in different environments, all being aerated.

3.6. Isothermal Titration Calorimetry Study. Isothermal titration calorimetry (ITC) has established itself to serve as an

dx.doi.org/10.1021/jp501150p | J. Phys. Chem. B 2015, 119, 2090−2102

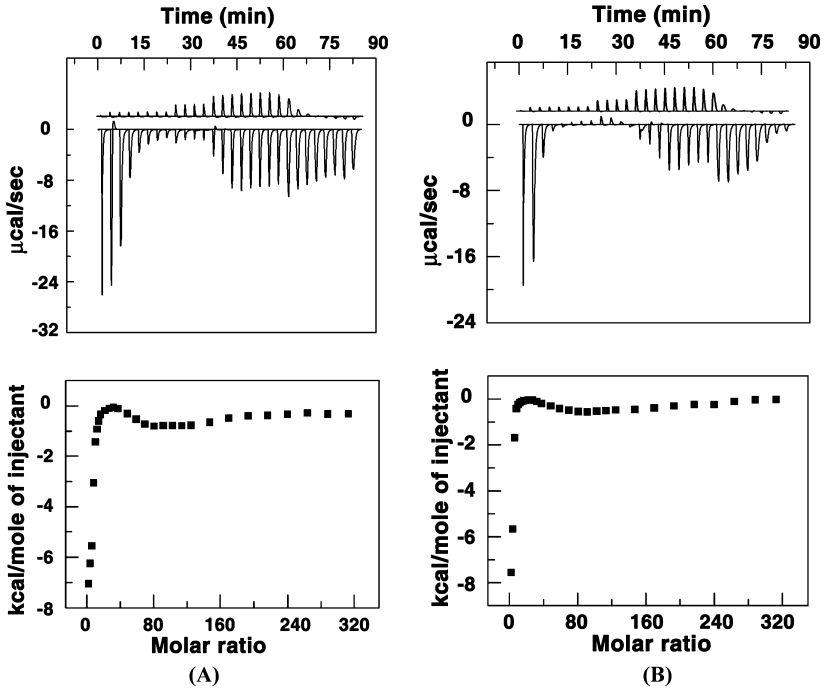

Figure 10. Top panel: ITC profile for the binding of SDS to (A) BSA and (B) HSA at 293 K in HEPES buffer, pH 7.0, indicating the raw data for sequential injection of SDS to the proteins. Bottom panel: Plot of integrated heat data after correction of heat of dilution of SDS against the molar ratio of SDS to protein.

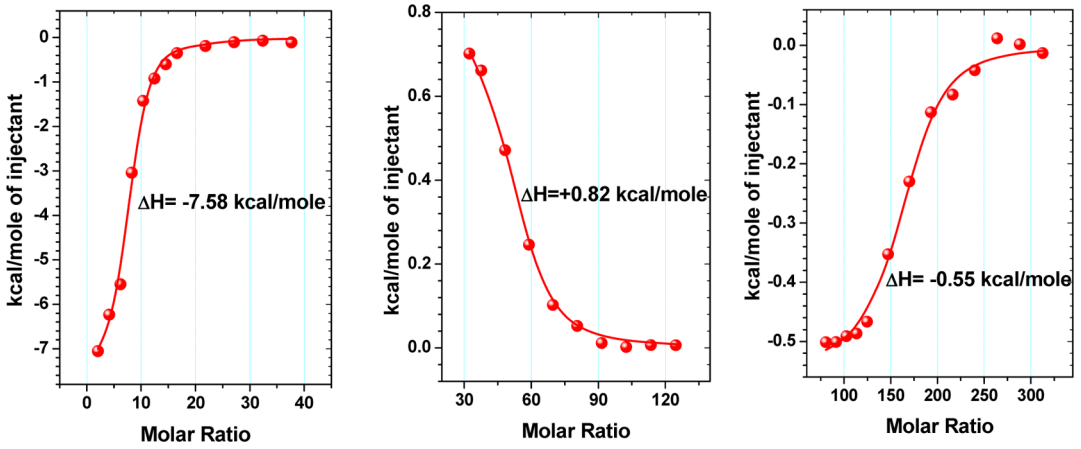

Figure 11. Plot of integrated heat data for BSA after correction of heat of dilution of SDS against the molar ratio of SDS to protein at pH 7.0. The data are fitted to a one-site model, and the solid curve represents the best fit.

effective tool to thermodynamically characterize the binding of small molecules, drugs, etc., to macromolecules.[50] Further, it provides significant insight into the energetics of the complexation process. Therefore, to investigate the stepwise unfolding of BSA and HSA by the action of SDS, we have performed the isothermal titration calorimetric measurements. As previous experiments indicate the unfolding is stepwise in nature, we expect different heat changes to occur during the different steps of the unfolding. In Figure 10 (top panel), the isothermal titration calorimetric data of the titration of SDS into the solutions of BSA and HSA are presented. Each injection heat burst curve in Figure 10 corresponds to a single injection. These injection heats are corrected by subtracting the corresponding dilution heats derived from the injection of identical amounts of SDS into buffer alone (Figure 10, top panel). Figure 10 reveals a typical ITC profile for the binding of SDS to the proteins. For both of the proteins, we observe three different regions of interaction with the surfactant.

For a better understanding of this stepwise interaction of SDS with the proteins and calculating the amounts of heat changes involved in each step, we have plotted integrated heat data against the molar ratio of SDS to the protein in three different molar ratio regions. Figure 11 reveals strong exothermic enthalpy changes at a relatively low molar ratio of SDS to BSA. Up to a molar ratio of 40, the interaction continues to be exothermic in nature and the amount of heat change (ΔH) is quite high, i.e., −7.58 kcal/mole. As we discussed earlier, in this region, interaction of SDS occurs in the specifically high energy sites of the protein. Thus, it is reasonable that in this region the value of ΔH should be higher. Previous workers have suggested that a low molar ratio of SDS can improve the thermal stability of BSA[51,52] as well as

dx.doi.org/10.1021/jp501150p | J. Phys. Chem. B 2015, 119, 2090−2102

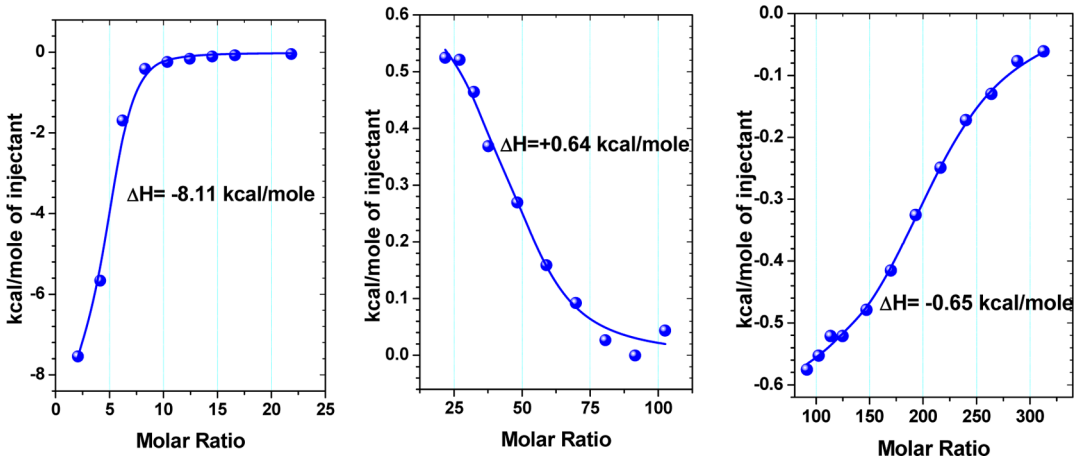

Figure 12. Plot of integrated heat data for HSA after correction of heat of dilution of SDS against the molar ratio of SDS to protein at pH 7.0. The data are fitted to a one-site model, and the solid curve represents the best fit.

other globular proteins.[53,54] The increased thermal stability of BSA is attributed to the fact that anionic surfactants bind more strongly to the native form of the protein than to the denatured form,[51,53] resulting in a high ΔH value. In the molar ratio region 40−120, the interaction is found to be endothermic in nature with a ΔH value of +0.82 kcal/mole, which is much lower compared to the heat involved in the previous region. In this region, interaction between protein and SDS is ascribed to be noncooperative. Beyond the molar ratio value 120, the interaction is again exothermic with a ΔH value of −0.55 kcal/mole, which can be attributed to the cooperative binding of SDS to the protein. A similar observation is also found for HSA (Figure 12), though the ΔH values in the three individual steps are different from those determined for BSA but the nature of interaction is the same as observed for BSA. ΔH values in each step of unfolding of both of the proteins with the addition of SDS are tabulated in Table 3. That for both BSA and HSA the

Table 3. ΔH Values for Each Step Obtained from ITC Study at pH 7.0

	step I (kcal/mole)	step II (kcal/mole)	step III (kcal/mole)
BSA	−7.58	+0.82	−0.55
HSA	−8.11	+0.64	−0.65

interaction is endothermic and spontaneous within the SDS/protein molar ratio 40−120 draws special attention. The process is ascribed to be entropy driven and is due to the removal of water molecules surrounding the nonpolar patches of the protein molecules. Release of counterions from the protein−surfactant assembly, in this second phase of interaction, is also an entropy driven process and might contribute to making the interaction spontaneous.

Ionic surfactants are reported to bind to BSA molecules through electrostatic and hydrophobic interactions.[55] Previous calorimetric studies have shown that the exothermic interaction between SDS and BSA is due to the binding of SDS to high affinity sites of the protein through a combination of both electrostatic and hydrophobic interactions.[56] However, no study is made to decipher the type of interaction occurring during the second step. Either electrostatic or hydrophobic interaction would be responsible for this endothermicity in the ITC profile for the binding of SDS to the proteins (Figure 10). This provokes us to explore the mode of interaction occurring in the second step of the unfolding of both of the serum albumins by SDS. The literature suggests at higher pH (pH > 5) serum albumins have a net negative charge, whereas at lower pH (pH < 5) they sustain a net positive charge.[57] To verify whether the second step involves electrostatic or hydrophobic interaction, we have performed the ITC experiment at lower pH, i.e., pH 3.1, as well. Figure 13 presents the ITC profile for the interaction of SDS with BSA and HSA at pH 3.1. At lower pH, we also observe a similar type of ITC profile as we have seen earlier at higher pH where only the absolute ΔH values differ. As done earlier, we have plotted integrated heat data against the molar ratio of SDS to the proteins in three different molar ratio regions (Figures 14 and 15). ΔH values in each step of interaction of SDS with both of the proteins are tabulated in Table 4.

At both of the pH's, the ITC experiments imply that the protein−SDS interaction takes place in three stages. The first one is assigned to the specific binding of SDS monomers to the high energy sites of the proteins, while the third step is ascribed to the cooperative binding between the two interacting partners.[34−37] To verify whether the second step involves electrostatic or hydrophobic interaction, we have performed the ITC experiments at pH 7.0 and 3.1. Had the electrostatic interaction constituted the second step of interaction between the serum proteins and negatively charged surfactant, the nature of the surface charge of these proteins should be the governing factor in this step. Again, as stated above, the nature of the surface charge of the serum proteins changes from negative to positive as the solution pH is changed from 7.0 to 3.1.[57] Thus, a change in the pH of the medium from 7.0 to 3.1 should have a prominent signature on the ITC profiles. However, it is evident from Figures 10 and 13 that the nature of interaction in the second step of unfolding hardly depends on the pH of the medium, although the extent of interactions, reflected by ΔH values tabulated in Tables 3 and 4, depend slightly on it. Thus, from the ITC experiments at two different pH's, we conclude that the interaction in the second step is hydrophobic in nature and electrostatic interaction plays no significant role in this step. The slight change in the ΔH values is likely due to the change in the buffer. The outcome of the ITC study corroborates the results of the spectroscopic measurements that unfolding of the serum albumins with the gradual addition of SDS occurs in a stepwise fashion. The study

dx.doi.org/10.1021/jp501150p | J. Phys. Chem. B 2015, 119, 2090−2102

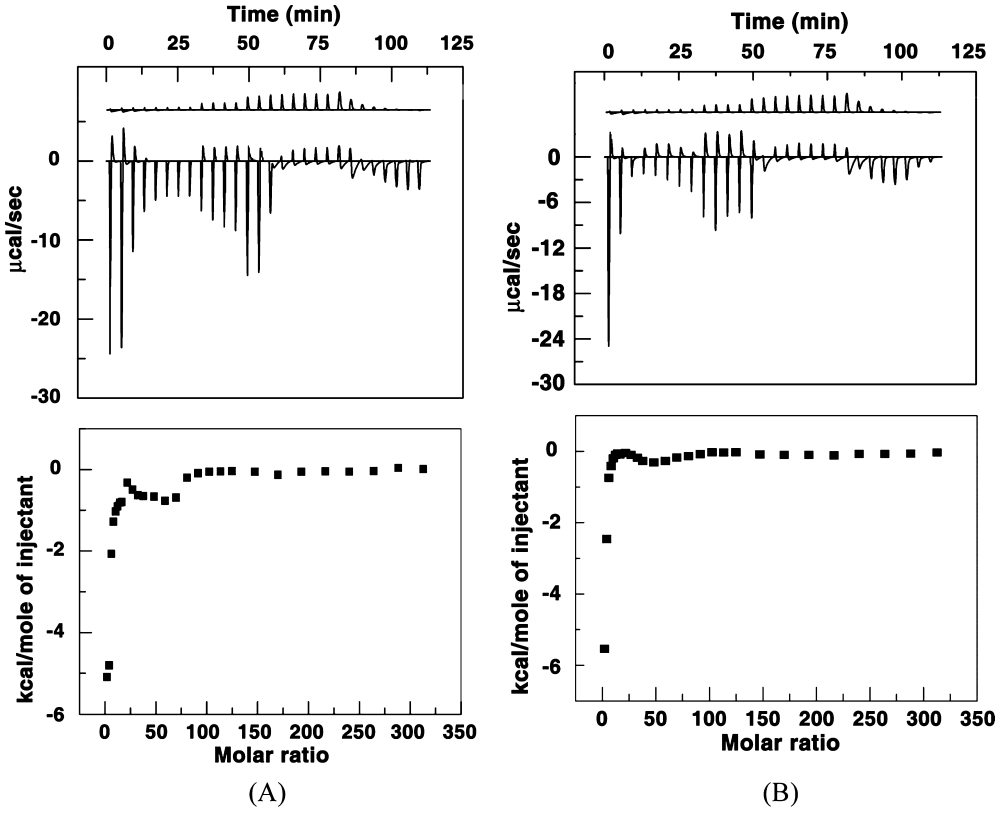

Figure 13. Top panel: ITC profile for the binding of SDS to (A) BSA and (B) HSA at 293 K in citric acid buffer, pH 3.1, indicating the raw data for sequential injection of SDS to the proteins. Bottom panel: Plot of integrated heat data after correction of heat of dilution of SDS against the molar ratio of SDS to protein.

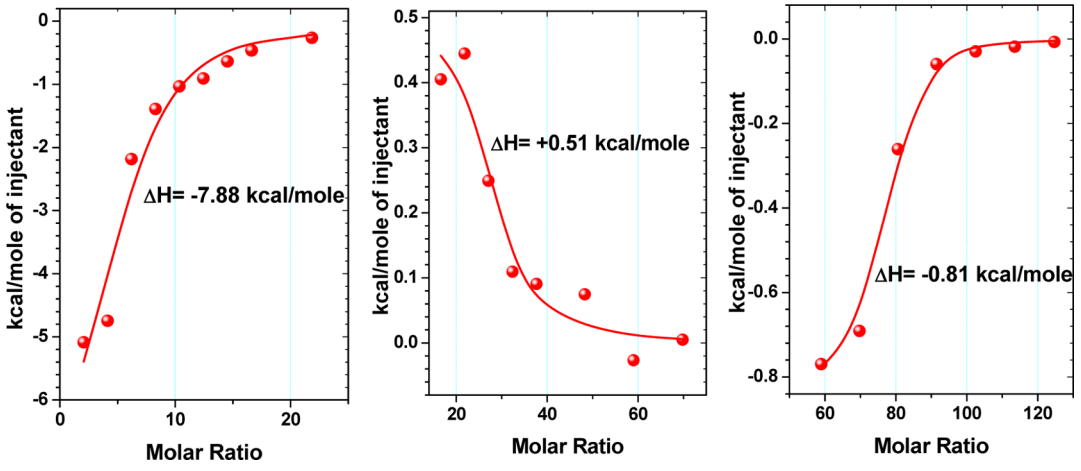

Figure 14. Plot of integrated heat data for BSA after correction of heat of dilution of SDS against the molar ratio of SDS to protein at pH 3.1. The data are fitted to a one-site model, and the solid curve represents the best fit.

further establishes that the second phase of interaction between the serum proteins and SDS is hydrophobic in nature.

As a general comment, the nature of the overall surfactant induced unfolding process of BSA and HSA is a reversible process though not totally.[58] Anand and Mukherjee have shown that BSA can be refolded from its unfolded state by the addition of β-cyclodextrin.[58] Their CD spectroscopic results reveal almost 100% recovery of the secondary structure lost during SDS induced unfolding. Retention of the secondary structure of the proteins to a good extent, as revealed from the CD spectra, confirms that even at high SDS concentration the serum proteins do not undergo complete denaturation.

4. CONCLUSION

Vivid steady-state and time-resolved fluorometric studies exploiting an external biological fluorophore, NHM, establish sequential unfolding of two major transport proteins, BSA and HSA, by the action of anionic surfactant SDS. A high concentration of SDS is found to unfold the serum proteins substantially to displace NHM from its binding sites in the proteins and to bind the probe with the micellar phase. Circular dichroism study reveals that at high SDS concentration the secondary structure of the proteins is lost significantly. Isothermal calorimetric study corroborates the proposition of

dx.doi.org/10.1021/jp501150p | J. Phys. Chem. B 2015, 119, 2090−2102

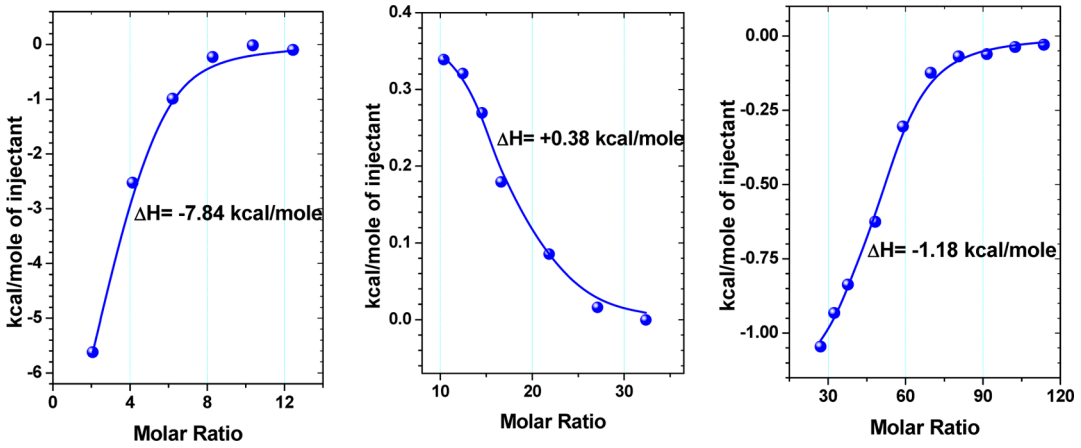

Figure 15. Plot of integrated heat data for HSA after correction of heat of dilution of SDS against the molar ratio of SDS to protein at pH 3.1. The data are fitted to a one-site model, and the solid curve represents the best fit.

Table 4. ΔH Values for Each Step Obtained from ITC Study at pH 3.1

	step I (kcal/mole)	step II (kcal/mole)	step III (kcal/mole)
BSA	−7.88	+0.51	−0.81
HSA	−7.84	+0.38	−1.18

stepwise unfolding of the serum proteins with the gradual addition of SDS and also measures the heat changes involved in the individual steps of the unfolding process. That the second step of the multistep unfolding process involves hydrophobic interaction has been established from the ITC experiments performed at two different pH's. The present work is expected to provide an important insight into the interaction and energetics of the serum proteins with anionic surfactants.

■ ASSOCIATED CONTENT

Supporting Information

Figures corresponding to the variation of the fluorescence anisotropies (r) of NHM (monitoring at 450 and 380 nm) against concentrations of both the proteins, plot for the determination of CMC of SDS in water and HEPES buffer, variation of the average lifetime of NHM in proteins with increasing molar ratio of SDS to the proteins, and variation of the $E_T(30)$ values in the vicinity of NHM in both the proteins against the molar ratio of SDS to the protein. This material is available free of charge via the Internet at http://pubs.acs.org.

■ AUTHOR INFORMATION

Corresponding Author

*Fax: 91-33-2414 6584. E-mail: nitin.chattopadhyay@yahoo.com.

Notes

The authors declare no competing financial interest.

■ ACKNOWLEDGMENTS

Financial support from the D.S.T. and D.B.T., Government of India, is gratefully acknowledged. S.G. and D.B. thank University Grants commission, Govt. of India, for their fellowships.

■ REFERENCES

(1) Peters, T. *All about Albumin; Biochemistry, Genetics and Medical Applications*; Academic Press: New York, 1995.
(2) Carter, D. C.; Ho, J. X. Structure of Serum Albumin. *Adv. Protein Chem.* **1994**, *45*, 153−176.
(3) Min, H. X.; Carter, D. C. Atomic Structure and Chemistry of Human Serum Albumin. *Nature* **1992**, *358*, 209−215.
(4) Peters, T. Serum albumin. *Advances in Protein Chemistry*; Academic Press: New York, 1985; Vol. *37*, pp 161−245.
(5) Helms, M. K.; Peterson, C. E.; Bhagavan, N. V.; Jameson, D. M. Time-resolved Fluorescence Studies on Site-directed Mutants of Human Serum Albumin. *FEBS Lett.* **1997**, *408*, 67−70.
(6) El-Kemary, M.; Gil, M.; Douhal, A. Relaxation Dynamics of Piroxicam Structures within Human Serum Albumin Protein. *J. Med. Chem.* **2007**, *50*, 2896−2902.
(7) Hu, Y.-J.; Liu, Y.; Xiao, X.-H. Investigation of Interaction between Berberine and Human Serum Albumin. *Biomacromolecules* **2009**, *10*, 517−521.
(8) Barreleiro, P. C. A.; Lindman, B. The Kinetics of DNA-Cationic Vesicle Complex Formation. *J. Phys. Chem. B* **2003**, *107*, 6208−6213.
(9) Demchenko, A. P. In *Topics in Fluorescence Spectroscopy: Biochemical Applications*; Lakowicz, J. R., Ed.; Plenum: New York, 1992; Vol. *3*, p 65.
(10) Cardenas, M.; Schillen, K.; Pebalk, D.; Nylander, T.; Lindman, B. Interaction between DNA and Charged Colloids Cloud Be Hydrophobically Driven. *Biomacromolecules* **2005**, *6*, 832−837.
(11) Haldar, B.; Chakrabarty, A.; Mallick, A.; Mandal, M. C.; Das, P.; Chattopadhyay, N. Fluorometric and Isothermal Titration Calorimetric Studies on Binding Interaction of a Telechelic Polymer with Sodium Alkyl Sulfates of Varying Chain Length. *Langmuir* **2006**, *22*, 3514−3520.
(12) Mallick, A.; Haldar, B.; Chattopadhyay, N. Spectroscopic Investigation on the Interaction of ICT Probe 3-acetyl-4-oxo-6,7-dihydro-12H indolo-[2,3- a]quinolozine with Serum Albumins. *J. Phys. Chem. B* **2005**, *109*, 14683−14690.
(13) Becker, R. S.; Ferreira, L. F. V.; Elisei, F.; Machado, I.; Latterini, L. Comprehensive Photochemistry and Photophysics of Land- and Marine-based β-carbolines Employing Time-resolved Emission and Flash Transient spectroscopy. *Photochem. Photobiol.* **2005**, *81*, 1195−1204.
(14) Chac, K. H.; Ham, H. S. Production of Singlet Oxygen and Super Oxide Anion Radicals by β-carbolines. *Bull. Korean Chem. Soc.* **1986**, *7*, 478−479.
(15) Duportail, G. Linear and Circular Dichroism of Harmine and Harmaline Interacting with DNA. *Int. J. Macromol.* **1981**, *3*, 188−192.
(16) Munoz, M. A.; Carmona, C.; Hidaigo, J.; Guaraldo, P.; Balon, M. Molecular Associations of Flavins with β-carbolines and Related Indoles. *Bioorg. Med. Chem.* **1995**, *3*, 41−47.
(17) Beljanski, M.; Beljanski, M. S. Three Alkaloids As Selective Destroyers of the Proliferative Capacity of Cancer Cells. *IRCS Med. Sci.* **1984**, *12*, 587−588.

(18) Reyman, D.; Vinas, M. H.; Poyato, J. M. L.; Pardo, A. Proton Transfer Dynamics of Norharman in Organic Solvents. *J. Phys. Chem. A* **1997**, *101*, 768−775.
(19) Varela, A. P.; Burrows, H. D.; Douglas, P.; Miguel, M. G. Triplet State Studies of β-carbolines. *J. Photochem. Photobiol., A* **2001**, *146*, 29−36.
(20) Vert, F. T.; Sanchez, I. Z.; Torrent, A. O. Acidity Constants of β-carbolines in the Ground and Excited Singlet State. *J. Photochem.* **1983**, *23*, 355−368.
(21) Mallick, A.; Chattopadhyay, N. Photophysics of Norharmane in Micellar Environments: A Fluorometric Study. *Biophys. Chem.* **2004**, *109*, 261−270.
(22) Chakrabarty, A.; Mallick, A.; Haldar, B.; Purkayastha, P.; Das, P.; Chattopadhyay, N. Surfactant Chain-length Dependent Modulation of Prototropic Transformation of a Biological Photosensitizer: Norharmane in Anionic Micelles. *Langmuir* **2007**, *23*, 4842−4848.
(23) Mallick, A.; Haldar, B.; Chattopadhyay, N. Encapsulation of Norharmane in Cyclodextrin: Formation of 1:1 and 1:2 Complexes. *J. Photochem. Photobiol., B* **2005**, *78*, 215−221.
(24) Chakrabarty, A.; Mallick, A.; Haldar, B.; Das, P.; Chattopadhyay, N. Binding Interaction of a Biological Photosensitizer with Serum Albumins: A Biophysical Study. *Biomacromolecules* **2007**, *8*, 920−927.
(25) Moriyama, Y.; Takeda, K. Re-formation of the Helical Structure of Human Serum Albumin by the Addition of Small Amount of Sodium Dodecyl Sulfate after the Disruption of the Structure by Urea. A Comparison with Bovine Serum Albumin. *Langmuir* **1999**, *15*, 2003−2008.
(26) Anand, U.; Jash, C.; Mukherjee, S. Spectroscopic Probing of the Microenvironment in a Protein-Surfactant Assembly. *J. Phys. Chem. B* **2010**, *114*, 15839−15845.
(27) De, S.; Girigoswami, A.; Das, S. Fluorescence Probing of Albumin-Surfactant Interaction. *J. Colloid Interface Sci.* **2005**, *285*, 562−573.
(28) Lakowicz, J. R. *Principles of Fluorescence Spectroscopy*, 3rd ed.; Springer: New York, 2006; Vol. *12*, p 578.
(29) Sinha, R.; Islam, M. M.; Bhadra, K.; Suresh Kumar, G.; Banerjee, A.; Maiti, M. The Binding of Intercalating and Non-intercalating Compounds to A-form and Protonated Form of Poly(rC). Poly(rG): Spectroscopic and Viscometric Study. *Bioorg. Med. Chem.* **2006**, *14*, 800−814.
(30) Giri, P.; Suresh Kumar, G. Self-structure Induction in Single Stranded Poly(A) by Small Molecules: Studies on DNA Intercalators, Partial Intercalators and Groove Binding Molecules. *Arch. Biochem. Biophys.* **2008**, *474*, 183−192.
(31) Islam, M. M.; Pandya, P.; Roy Chowdhury, S.; Kumar, S.; Suresh Kumar, G. Binding of DNA-binding Alkaloids Berberine and Palmatine to tRNA and Comparison to Ethidium: Spectroscopic and Molecular Modeling Studies. *J. Mol. Struct.* **2008**, *891*, 498−507.
(32) Mallick, A.; Chattopadhyay, N. Photophysics in Motionally Constrained Bioenvironment: Interaction of Norharmane with Bovine Serum Albumin. *Photochem. Photobiol.* **2005**, *81*, 419−424.
(33) Santra, M. K.; Banerjee, A.; Rahaman, O.; Panda, D. Unfolding Pathways in Human Serum Albumin, in: Evidence for Sequential Unfolding and Folding of Its Three Domains. *Int. J. Biol. Macromol.* **2005**, *37*, 200−204.
(34) Gelamo, E. L.; Tabak, M. Spectroscopic Studies on the of Bovine (BSA) and Human (HSA) Serum Albumins with Ionic Surfactants. *Spectrochim. Acta, Part A* **2000**, *56*, 2255−2271.
(35) Tanford, C. *The Hydrophobic Effect: formation of micelles and biological membranes*, 2nd ed.; Wiley-Interscience: New York, 1986.
(36) Reynolds, J. A.; Tanford, C. Binding of Dodecyl Sulfate to Proteins at High Binding Ratios. Possible Implications for the State of Proteins in Biological Membranes. *Proc. Natl. Acad. Sci. U.S.A.* **1970**, *66*, 1002−1007.
(37) Li, Y.; Wang, X.; Wang, Y. Comparative Studies on Interactions of Bovine Serum Albumin with Cationic Gemini and Single-Chain Surfactants. *J. Phys. Chem. B* **2006**, *110*, 8499−8505.
(38) Oshima, J.; Shiobara, S.; Naoumi, H.; Kaneko, S.; Yoshihara, T.; Mishra, A. K.; Tobita, S. Extreme Fluorescence Sensitivity of Some Aniline Derivatives to Aqueous and Nonaqueous Environments: Mechanistic Study and Its Implication as a Fluorescent Probe. *J. Phys. Chem. A* **2006**, *110*, 4629−4637.
(39) Matzinger, S.; Hussey, D. M.; Fayer, M. D. Fluorescent Probe Solubilization in the Headgroup and Core Regions of Micelles: Fluorescence Lifetime and Orientational relaxation Measurements. *J. Phys. Chem. B* **1998**, *102*, 7216−7224.
(40) Draxler, S.; Lippitsch, M. E. Excited-State Acid-Base Kinetics and Equilibria in Norharman. *J. Phys. Chem.* **1993**, *97*, 11493−11496.
(41) Hong, M.; Weekley, B. S.; Grieb, S. J.; Foley, J. P. Electrokinetic Chromatography Using Thermodynamically Stable Vesicles and Mixed Micelles Formed from Oppositely Charged Surfactants. *Anal. Chem.* **1998**, *70*, 1394−1403.
(42) Kosower, E. M.; Dodiuk, H.; Tanizawa, K.; Ottolenghi, M.; Orbach, N. Intramolecular Donor-Acceptor Systems. Radiative and Nonradiative Processes for the Excited States of 2-*N*-Arylamino-6-Naphthalenesulfonates. *J. Am. Chem. Soc.* **1975**, *97*, 2167−2178.
(43) Reichardt, C. In *Molecular Interactions*; Ratajazak, H., Orville Thomas, W. J., Eds.; Wiley: New York, 1982; Vol. *3*.
(44) Bose, D.; Ghosh, D.; Das, P.; Girigoswami, A.; Sarkar, D.; Chattopadhyay, N. Binding of a Cationic Phenazinium Dye in Anionic Liposomal Membrane: A Spectacular Modification in the Photophysics. *Chem. Phys. Lipids* **2010**, *163*, 94−101.
(45) Mahata, A.; Sarkar, D.; Bose, D.; Ghosh, D.; Girigoswami, A.; Das, P.; Chattopadhyay, N. Photophysics and Rotational Dynamics of a β-carboline Analogue in Nonionic Micelles: Effect of Variation of Length of the Head Group and the Tail of the Surfactant. *J. Phys. Chem. B* **2009**, *113*, 7517−7526.
(46) Moriyama, Y.; Takeda, K. Protective Effects of Small Amounts of Bis(2-ethylhexyl)sulfosuccinate on the Helical Structures of Human and Bovine Serum Albumins in Their Thermal Denaturations. *Langmuir* **2005**, *21*, 5524−5528.
(47) Parker, W.; Song, P. S. Protein Structures in SDS Micelle-Protein Complexes. *Biophys. J.* **1992**, *61*, 1435−1439.
(48) Sengupta, B.; Sengupta, P. K. Binding of Quercetin with Human Serum Albumin: A Critical Spectroscopic Study. *Biopolymers* **2003**, *72*, 427−434.
(49) Takeda, K.; Moriyama, Y. Comment on the Misunderstanding of the BSA-SDS Complex Model: Concern about Publications of an Impractical Model. *J. Phys. Chem. B* **2007**, *111*, 1244.
(50) Giri, P.; Kumar, G. S. Binding of Protoberberine Alkaloid Coralyne with Double Stranded Poly(A): A Biophysical Study. *Mol. BioSyst.* **2008**, *4*, 341−348.
(51) Deep, S.; Ahluwalia, J. C. Interaction of Bovine Serum Albumin with Anionic Surfactants. *Phys. Chem. Chem. Phys.* **2001**, *3*, 4583−4591.
(52) Giancola, C.; De Sena, C.; Fessas, D.; Graziano, G.; Barone, G. DSC Studies on Bovine Serum Albumin Denaturation. Effect of Ionic Strength and SDS Concentration. *Int. J. Biol. Macromol.* **1997**, *20*, 193−204.
(53) Magdassi, S.; Vinetsky, Y.; Relkin, P. Formation and Structural Heat-stability of β-Lactoglobulin/Surfactant Complexes. *Colloids Surf., B* **1996**, *6*, 353−362.
(54) Waninge, R.; Paulsson, M.; Nylander, T.; Ninham, B.; Sellers, P. Binding of Sodium Dodecyl Sulfate and Dodecyl Trimethyl Ammonium Chloride to β-Lactoglobulin: A Calorimetric Study. *Int. Dairy J.* **1998**, *8*, 141−148.
(55) Kelley, D.; McClements, D. Interactions of Bovine Serum Albumin with Ionic Surfactants in Aqueous Solutions. *J. Food Hydrocolloids* **2003**, *17*, 73−85.
(56) Nielsen, A. D.; Borch, K.; Westh, P. Thermochemistry of the Specific Binding of C12 Surfactants to Bovine Serum Albumin. *Biochim. Biophys. Acta* **2000**, *1479*, 321−331.
(57) Böhme, U.; Scheler, U. Effective Charge of Bovine Serum Albumin Determined by Electrophoresis NMR. *Chem. Phys. Lett.* **2007**, *435*, 342−345.
(58) Anand, U.; Mukherjee, S. Reversibility in Protein Folding: Effect of β-cyclodextrin on Bovine Serum Albumin Unfolded by Sodium Dodecyl Sulphate. *Phys. Chem. Chem. Phys.* **2013**, *15*, 9375−9383.